Article │ Received 26 January 2026; Revised 3 May 2026; Accepted 22 May 2026; Published 29 June 2026
https://doi.org/10.55092/sc20260013

A probabilistic digital twin framework for corrosion-fatigue prognosis of floating offshore wind turbines

Yasmin Ali[1,2], Ahmed Elgammal[1], Chengjun Li[3], Junlin Heng[1,*] and Kaoshan Dai[1,4]

[1] Department of Civil Engineering, Sichuan University, Chengdu 610065, China
[2] Department of Civil Engineering, Delta University for Science and Technology, Gamasa 11152, Egypt
[3] Sichuan Transportation Research Institute, Sichuan Vocational and Technical College of Communications, Chengdu 611130, China
[4] State Key Laboratory of Intelligent Construction and Healthy Operation and Maintenance of Deep Underground Engineering, Sichuan University, Chengdu 610065, China

* Correspondence author; E-mail: junlin.heng@scu.edu.cn.

Highlights:

- Probabilistic digital twin framework for corrosion-fatigue prognosis.
- Bayesian inference updates multi-phase physics models using online sensor data.
- Applied to floating offshore wind turbine towers under stochastic loads.
- Condition-based strategy reduces lifecycle maintenance costs by roughly 65%.
- Probabilistic maintenance oversight reduces operational downtime by 58%.

Abstract: Floating offshore wind turbines face growing integrity-management challenges caused by coupled corrosion and fatigue in harsh marine environments. Existing digital-twin frameworks are not yet well suited to combine multi-phase degradation physics with dynamic uncertainty quantification for this problem. To address this gap, this paper proposes a probabilistic digital twin framework that integrates sensor data acquisition, multi-physics simulation, and Bayesian inference for corrosion-fatigue prognosis. A three-phase damage evolution model is formulated to represent the transition from corrosion pitting to short-crack growth and long-crack propagation. Operational observations are assimilated recursively to update fatigue parameters and remaining useful life estimates. The framework is demonstrated using the IEA 15 MW reference wind turbine. The updated model identifies the onset of accelerated crack propagation at year 20 and reduces the 95% remaining-useful-life confidence interval from 40.4 years to 3.4 years. A maintenance strategy based on the updated failure probability reduces operational downtime by 58% and lifecycle cost by approximately 64.9% compared with a fixed-interval strategy. The results indicate that probabilistic updating can support more transparent inspection and maintenance decisions for floating offshore wind turbine structures under corrosion-fatigue degradation.

Keywords: floating offshore wind turbine; corrosion-fatigue; digital twins; structural health monitoring; condition-based maintenance; prognostic health management; remaining useful life; Bayesian inference

1. Introduction

Wind energy is seen as one of the key means for the world to reduce the carbon emissions and is projected to produce over 30% of global electricity by 2050, which would lead to an annual decrease of CO_2 emissions of around 14,871 million tons [1–3]. Although historically, onshore methods have been the accessible choice, the wind industry steps a new route to sea due to the need for high-quality wind resources and the threatening shortage of the available land sites [4,5]. However, as water depths exceed 60 m (where 80% of the global offshore wind resources are located) traditional fixed-bottom offshore wind structures are no longer technically or economically feasible [6,7]. Hence, floating offshore wind turbines are viewed as the necessary technological innovation for the commercialization of deep-water offshore sites. These turbines have the added benefits of improving wind resources since they can be moored further from shore and benefit from stronger and more consistent winds, as well as reducing visual and acoustic impacts compared to near-shore fixed-bottom structures [8,9].

However, the floating offshore wind turbines are largely constrained by excessive operation and maintenance (O&M) costs, which makes the economic model difficult to realize. The O&M costs make up 20%–25% of the levelized cost of energy in wind power systems with logistics factors causing up to 57% of this outlay depending on variables like distance to shore and water depth [10–12]. The economic burden is increased by the weather's impact on the service vessels, e.g., the service vessels have to be secured and hence require good weather. For example, the combination of strong waves and high wind speeds can make it unsafe for crew boats to operate and reach the site facility. Similarly, these loads can also cause the available maintenance windows to decrease by almost 5% thereby complicating logistics and the risk of turbine downtimes due to the inaccessibility goes up [13,14]. Furthermore, the expansion of offshore deployment increased transit times and the fuel burn, thus incorporating larger and specific vessels while promoting smart route optimization to contain the escalating logistical costs [15,16].

To solve these economic and logistical inefficiencies, the industry is more and more shifting from reactive, corrective maintenance methods to predictive, condition-based maintenance (CBM). While corrective maintenance leads to high costs as a result of unplanned downtime and emergency mobilization of heavy-lift vessels, CBM uses condition monitoring to facilitate early intervention before catastrophic failure [17,18]. Empirical evidence shows that the implementation of advanced CBM methods can cut direct O&M costs by up to 8% and yearly maintenance costs by some 32% to 39% compared to traditional corrective methods [18,19]. By correctly optimizing inspection intervals based on the actual degradation status of critical components, CBM reduces production losses and optimizes the utilization of restricted weather windows. Hence, CBM creates a critical path to lowering the general levelized cost of energy of floating offshore wind projects [17,20].

Among the components of floating offshore wind turbines, the tower base is identified as highly vulnerable to cumulative fatigue damage. Differently from its fixed-bottom counterpart, the tower base of a floating platform is in the superposition of high-cycle axial stresses originating from aerodynamic thrust and low-frequency bending moments exerted by hydrodynamic wave excitations [21,22]. Such vulnerability is exacerbated in the splash zone, where the structure is constantly exposed to alternating wetting and drying cycles, which increase the rate of electrochemical degradation [23,24]. Moreover, the tower base is also subjected to the largely unpredictable mechanical loads due to the directional variability of wind and waves as well as to the severe corrosiveness of the saline marine environment.

Mechanical fatigue and chemical corrosion hereby combine to jeopardize the overall integrity of the tower base [25,26].

The development of material degradation in such environments can be roughly regarded as a non-linear transition from electrochemical degradation on the surface to mechanical degradation in the form of fractures. In the early stage, local anodic dissolution causes the formation of corrosion pits. These pits will subsequently be stress concentrators, and mechanical stretching at these locations will lead to cracks initiated at the edge of pitting [27,28]. After the cracks are formed, their advancement will be substantially influenced by the variable amplitude loading. The interaction between the different loading sequences and the overloads can cause to unexpected increase the crack growth rates mainly due to variation in the plastic zone created by the crack [29,30]. The co-action of corrosion and mechanical loading (corrosion-fatigue) highlights that the current linear summation of damage is not able to realistically estimate the loss of material life, as well as to model in the proper way the dynamics in the processes of pitting corrosion and fatigue crack growth under variable environmental loading [31,32].

Apart from the physical complexity, the environmental performance and their induced material behavior present significant uncertainty. Concerning environmental conditions, fatigue life predictions are deeply sensitive to random waves and salinity changes, which will affect the corrosion-fatigue crack advance through variations in the electrochemical activity in the crack vicinity [33,34]. In the other aspect, uncertainties concerning material databases (fatigue resistance scatter, weld geometry) can lead to substantially different results compared to theoretically predicted values [35,36]. Changes in input values can cause differences in the estimated fatigue resistance [37]. Consequently, the actual design life based exclusively on static deterministic models is considered more and more inappropriate [34,38].

Data-driven approaches, especially those leveraging deep learning, have emerged as promising alternatives to traditional deterministic modeling for structural health monitoring and prognosis. These methods excel at detecting intricate, non-linear relationships without requiring explicit physical laws. However, their use in offshore wind energy faces major hurdles due to limited data availability. Effective deep learning models demand extensive, high-quality datasets that include labeled failure instances. Such resources are scarce in this sector. The offshore wind industry struggles to compile such datasets because of high reliability standards and the relatively recent deployment of floating platforms [39,40], resulting in few recorded failure cases suitable for training. Moreover, harsh marine conditions often compromise sensor performance, leading to incomplete or noisy measurements. This makes it difficult to differentiate real structural deterioration from artifacts caused by sensor malfunctions [41,42]. While strategies like semi-supervised learning and synthetic data generation have been proposed to mitigate data shortages, purely data-dependent models often fail to generalize across different turbine configurations or damage types, undermining the accuracy of prognostic predictions when applied beyond their initial scope [43,44].

In response to these challenges, particularly in environments with limited operational data, the industry has increasingly adopted the digital twin concept as a holistic solution for system integration. Unlike fixed numerical models, a digital twin functions as a living virtual replica that evolves alongside its physical counterpart by integrating real-time sensor inputs. This enables capabilities such as virtual sensing and predictive diagnostics [45–47]. Although the digital twin framework allows for the fusion of physics-based simulations with empirical data, its application in real-time fatigue assessment is often hindered by high computational demands and the rigidity of conventional physical models. While

traditional physics-based twins are grounded in solid mechanical principles, they typically lack the adaptive capacity to account for evolving material degradation and variable environmental loads. Without continuous updating of uncertain parameters, these models can produce significant prediction errors [48,49]. Consequently, the performance of a digital twin relies on the fidelity of its underlying simulations and on its ability to assess and minimize uncertainty through iterative model calibration [50].

To meet the need for adaptability, Bayesian inference offers a solid mathematical framework for integrating sparse inspection data into physics-based fatigue models [51]. By treating key parameters (e.g., crack growth coefficients) as stochastic variables with evolving probability distributions, Bayesian approaches enable digital twins to be continuously refined as new information arrives [52,53]. This iterative updating is especially valuable in offshore wind settings, where sensor noise and changing environmental conditions can undermine the reliability of fixed parameter estimates. As real-time measurements are incorporated, the posterior distributions of degradation parameters grow more accurate, leading to reduced uncertainty in predictions of remaining useful life [54,55].

While such probabilistic methods have been extensively tested and validated for mechanical fatigue monitoring, their extension to combined corrosion-fatigue scenarios remains an emerging area. Significant progress has been achieved in assessing drivetrain and blade components, where digital twins that combine torsional dynamic models with hybrid physics-informed machine learning have successfully estimated both fatigue damage and remaining lifespan [45,48,56]. Nevertheless, fewer established frameworks exist for modeling the coupled corrosion-fatigue degradation of support structures. Recent efforts show promise: artificial intelligence (AI)-powered digital twins for tower bases now employ Gaussian processes to model interactions between corrosion and fatigue [51]. Moreover, adaptive control strategies based on time-dependent probabilistic models have been proposed to improve corrosion-fatigue reliability in ring-flange joints [57]. Other studies have integrated finite element simulations with machine learning for lattice-tubular towers, demonstrating the feasibility of combining structural health monitoring data with probabilistic assessments of corrosion-fatigue progression [58].

Despite these advances, a notable gap persists between detailed degradation modeling and practical economic decision-making in floating wind energy. Many existing approaches rely either on data-heavy AI techniques or simplified linear damage accumulation rules, which often fail to capture complex electrochemical behaviors, such as the shift from pitting corrosion to crack growth, that are crucial in splash zone failures. Furthermore, while probabilistic risk assessments are increasingly used, few studies effectively link Bayesian updating of multi-phase physical parameters with maintenance planning optimization through utility theory. Consequently, there is a clear need for a probabilistic digital twin framework capable of accurately representing the nonlinear physics of corrosion-fatigue interactions and directly translating updated risk estimates into cost-efficient, reliability-driven maintenance strategies for floating offshore wind turbines.

To address this challenge, the study presents a probabilistic digital twin framework designed to support the lifecycle management of floating offshore wind turbines subject to combined corrosion and fatigue degradation. The innovation lies in combining a multi-phase damage evolution model, which captures the transition from corrosion pitting to fatigue crack growth, within a recursive Bayesian inference system. The framework dynamically integrates real-time operational sensor data. This continuous input refines the probability distributions of critical fatigue parameters, thereby reducing uncertainty in remaining life estimates. A decision-support module, grounded in Bayesian decision

theory, is also included to evaluate maintenance options quantitatively and optimize inspection scheduling. The approach is illustrated through a case study based on the IEA 15 MW reference turbine mounted on a semi-submersible platform, offering a physics-informed strategy to enhance structural reliability, especially in data-scarce marine settings.

The paper is structured as follows: Section 2 outlines the digital twin architecture, focusing on the multi-phase corrosion-fatigue process and the mathematical basis for Bayesian updating. Section 3 presents the case study, detailing the turbine model setup, simulated crack propagation scenarios, and a comparison of different maintenance approaches. Section 4 concludes with a summary of key results and a discussion of the framework's potential impact on offshore wind asset management.

2. Probabilistic digital twin framework for corrosion-fatigue lifecycle management

2.1. Framework architecture and operational strategy

The proposed digital twin framework is designed to be modular and adaptive, integrating physical principles with actual operational conditions. As illustrated in Figure 1, the system operates through three interconnected, hierarchical stages (data acquisition, probabilistic modeling, decision support) that function within a continuous feedback loop. This approach supports two-way data exchange: sensor inputs are used to refine degradation models, while revised risk estimates inform and improve inspection strategies.

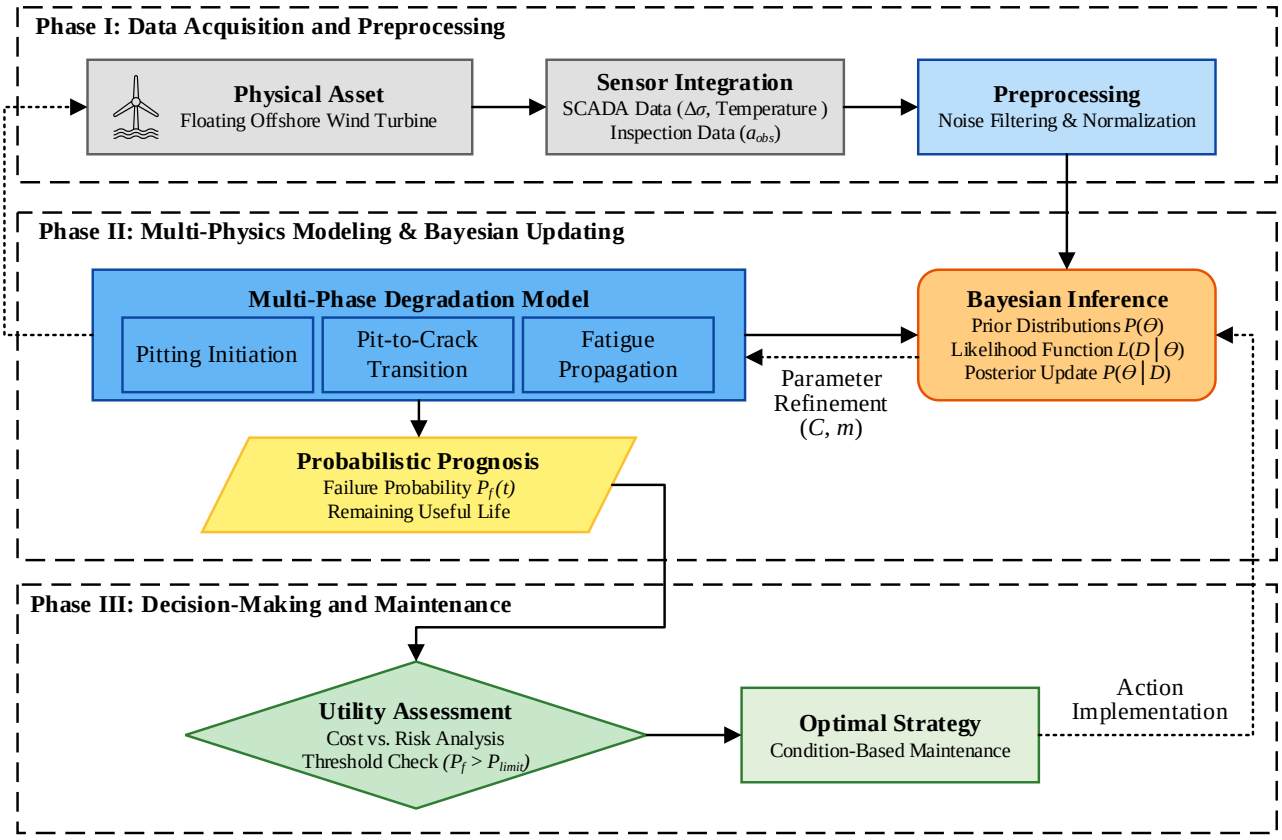

Figure 1. Architecture of the proposed probabilistic digital twin framework.

While definitions of digital models, digital shadows, and digital twins differ across engineering fields, recent efforts have converged on three essential characteristics of a true digital twin: a physical asset, its virtual representation, and real-time, bidirectional communication between them. Under this classification, a digital model involves manual data transfer, and a digital shadow allows automated data flow from the physical to the virtual side but lacks feedback in the reverse direction. A full digital twin, however, requires automated, two-way interaction to support lifecycle optimization [59,60]. In this framework, sensor data continuously updates the degradation model using Bayesian inference, and the resulting risk evaluations shape maintenance and inspection planning. Although the physical feedback occurs through scheduled human-led interventions rather than direct autonomous actuation, the seamless, automated exchange of data, model refinement, and decision-making ensures synchronized lifecycle management. Consequently, the system goes beyond the constraints of a one-directional digital shadow and meets the recognized criteria for a digital twin in structural asset management.

The very first step in the entire operation is the gathering of basic environmental and structural data (Phase I). Subsequently, the data is used in Bayesian multi-physics simulations to bring about the model correction (Phase II). The revised models then play an important role in the formulation of effective maintenance plans (Phase III).

Central to the computational kernel in Phase II is the detailed, multi-phase characterization of corrosion-fatigue deterioration. This characterization is the starting point for the selected probabilistic modeling strategy. The damage development process is segmented into three distinct sections: (i) corrosion-driven phase; (ii) competition phase; and (iii) fatigue-driven phase. The initial corrosion-driven phase is mainly run by electrochemical processes at the microscale level. In this time, the surface irregularities and stress concentrators promote the crack initiation. The increase in this area is determined by the effects of environmental and mechanical factors [61]:

$$\frac{da_{s1}}{dt} = \left(\frac{da_{s1}}{dt}\right)_c + \left(\frac{da_{s1}}{dt}\right)_f \tag{1}$$

where a_{s1} represents the length of the micro-crack, t stands for time, and the subscripts c and f correspond to the crack growth contributions from corrosion and fatigue, respectively. Once the defect grows beyond microscopic scales, the system enters the competition phase; a crucial stage in which further propagation depends on whichever driving mechanism prevails, whether it be electrochemical dissolution or mechanical fracture processes [62]:

$$\frac{da_{s2}}{dt} = \max\left[\left(\frac{da_{s2}}{dt}\right)_c, \left(\frac{da_{s2}}{dt}\right)_f\right] \tag{2}$$

where a_{s2} represents the crack length during the propagation phase. In this intermediate stage, fatigue behavior is described using fracture mechanics concepts applied to cracks larger than the effective initial flaw size (a_{EIFS}), determined from the fatigue threshold (ΔK_{th}) and the threshold stress range ($\Delta\sigma_L$) [63]:

$$a_{EIFS} = \frac{1}{\pi}\left(\frac{\Delta K_{th}}{Y_{fcg} \cdot \Delta\sigma_L}\right)^2 \tag{3}$$

where Y_{fcg} is the geometric correction factor related to the crack's configuration. When the crack reaches critical dimensions at which mechanical driving forces become dominant, damage progression

transitions into the fatigue-driven regime. In this phase, crack growth accelerates according to the Paris law, which expresses the propagation rate as a function of the stress intensity factor range (ΔK) [64,65]:

$$\left(\frac{da_{S2}}{dt}\right)_f = C \cdot (\Delta K - \Delta K_{th})^m \quad (4)$$

where C and m are material-specific constants that describe the resistance to fatigue crack growth. By integrating these governing equations into the probabilistic framework illustrated in Figure 1, the digital twin automatically shifts between different crack propagation mechanisms in response to changing stress conditions and environmental severity. This ensures that predicted service life accurately captures the intricate, non-linear physical behavior occurring in the splash zone.

2.2. Data integration and probabilistic preprocessing

The digital twin's operation relies on the thoughtful integration and refinement of multiple data streams. These data streams are the empirical basis for the probabilistic updates executed in Phase II. As proposed in Phase I (see Figure 1), the framework unites three main groups of input data: environmental parameters (e.g., wave kinematics, wind velocity, current profiles, salinity, temperature), operational loading histories (e.g., rotor speed, blade pitch, tower-base loads), and direct structural health observations (e.g., corrosion depth, crack length measurements, surface deformation). Environmental and operational telemetry are obtained from metocean sensors and supervisory control and data acquisition (SCADA) systems, respectively, while damage indicators are gained through the specific non-destructive evaluation (NDE) inspections. These measurements are sent to a land-based processing center that provides a clear and accurate overview of the turbine's health status.

Environmental and operational data substituting the acquisition of stress range through pre-computed load libraries, analytical models, or other high fidelity simulations done offline in the processing center. Instead of strain measurement with conversion to stress ranges, which is technical and applied in some structural health monitoring applications, the marine environment causes a lot of difficulties regarding sensor durability and long-term data reliability. For this reason, the proposed framework is mainly meant to work with stress ranges derived from environmental and operational telemetry via pre-computed load libraries or simplified analytical models, while strain-based measurements are used only as validation data for the method in case such are available. Thus, there is no need for real-time high-fidelity finite element or computational fluid dynamics (CFD) analyses within the probabilistic kernel, which results in precise load characterization alone. The resulting stress ranges and environmental parameters are then directly related to the micro-crack growth variable as1: the stress range $\Delta\sigma$ acts as the driving force for the fatigue componen das1dtf in Equation (1) and for the stress intensity factor range ΔK in Equation (4), while the monitored environmental conditions determine the electrochemical corrosion rate that governs the pitting term das1dtc.

Before being fed into the multi-physics kernel, raw sensor data go through a preprocessing phase aimed at minimizing measurement inconsistencies and aligning data into uniform formats. High-frequency noise in operational stress signals is suppressed using low-pass filters, while missing or broken segments are reconstructed via interpolation techniques, producing smooth, continuous load histories over time. For compatibility with Bayesian inference, point measurements from sensors are translated into probabilistic likelihood functions, incorporating known uncertainties and sensor precision. A

normalization step ensures that these processed observations align mathematically with the prior distributions of material properties, improving the stability of posterior updates. This stage effectively reduces inherent randomness in the input data by converting raw telemetry into refined, probabilistic representations. The model tracks degradation using Monte Carlo sampling, allowing quick, frequent updates to failure probability and remaining useful life predictions, which align well with maintenance scheduling needs.

2.3. Bayesian inference and prognostic modeling

The damage evolution of the multi-phase model presented in Section 2.1 is deterministic, however, the digital twin's predictive precision is basically restricted by the epistemic uncertainties regarding material constants and environmental conditions. The framework, to deal with this problem, is comprised of a recursive Bayesian inference module (Phase II in Figure 1) that functions iteratively to update the governing fatigue parameters (*i.e.*, the Paris law coefficient (C) and exponent (m)) depending on the model deviation between the predicted and real-time observed crack growth. The parameters are treated as stochastic variables ($\theta = \{C, m\}$) nd the system updates the reference probability distributions when new inspection data (D) is available, henceforth according to Bayes' theorem [66]:

$$P(\theta|D) = \frac{P(D|\theta)P(\theta)}{P(D)} \tag{5}$$

where $P(\theta)$ is the prior distribution, $P(D|\theta)$ is the likelihood of observing data D for a given parameter set θ, and $P(\theta|D)$ is the posterior distribution. The likelihood is formulated from the deviation between the observed crack size ($a_{obs,i}$) and the model-predicted crack size ($a_{model,t}$), assuming a Gaussian observation error with standard deviation σ_{obs}, as expressed in Equation (6). Parameter sets that reproduce the inspection observations more closely therefore receive higher posterior probability, progressively narrowing the prediction interval.

$$P(D|\theta) \propto \exp\left(-\frac{1}{2\sigma_{obs}^2}\sum_{i=1}^{n}\left(a_{obs,i} - a_{model,t}(\theta)\right)^2\right) \tag{6}$$

To address the potential for false negatives in marine settings, the likelihood function $P(D|\theta)$ can be expanded to include a detection probability curve $PoD(a)$ [67–69]. Under these conditions, the likelihood associated with an inspection event takes the form of a mixture model.

$$P(D|\theta) = \prod_{i=1}^{N}\left[PoD\left(a_{model,i}\right)\cdot\mathcal{N}\left(a_{obs,i}|a_{model,i},\sigma_{obs}\right) + \left(1 - PoD\left(a_{model,i}\right)\right)\cdot\mathbb{I}\left(a_{obs,i} = 0\right)\right] \tag{7}$$

where $\mathbb{I}(\cdot)$ is a null observation (no crack detected) indicator function. Through this mechanism, the Bayesian updater can incorporate the previous case of a crack existing but missed due to biofouling or visibility constraints, preventing over-confident belief in no-damage state.

The subsequent step is the Bayesian update; the posterior distributions of C and m are transferred to the physics kernel by means of Monte Carlo simulations in order to obtain the temporally varying probability of failure ($P_f(t)$). The failure event is defined as the case where the actual depth of crack ($a(t)$) exceeds the critical limit decided by component geometry (a_{cr}). Therefore, the failure probability in total is evaluated as [65]:

$$P_f(t) = P\left[\bigcup_{i=1}^{N_{sim}} G_i(t) < 0\right] \tag{8}$$

$$G_i(t) = a_{cr} - a_i(t) \tag{9}$$

where $G_i(t)$ is the limit state function for the i-th simulation iteration, and Nsim is the total amount of Monte Carlo samples. Such output in terms of probability is further utilized in risk-informed decision-making reasoning detailed later.

2.4. Utility-based decision making

The last module of the structure of the framework (Phase III in Figure 1) shifts from probabilistically based prognostics into the practical maintenance strategies through the help of Bayesian decision theory. This stage is meant to settle the dilemma over the immediate costs arising from the intervention and the long-term losses that may be caused by the structural failure. The consequences of numerous maintenance strategies, e.g., regular inspections or direct repairs, are assessed, and the optimal plan, which would raise the expected utility under uncertainty, is selected by the system [70]. The expected utility (EU) for the given maintenance action (A) is developed as the sum of the utilities of all possible outcomes weighed by their respective probabilities:

$$EU(A) = \sum_i P(O_i|A) \cdot U(O_i) \tag{10}$$

where $P(O_i|A)$ denotes the posterior probability of outcome O_i, such as safe operation, minor repair, or catastrophic failure, conditional on action A, and $U(O_i)$ is the utility assigned to that outcome, including direct cost, downtime, and safety consequences.

The present framework provides the conditional outcome probabilities $P(O_i|A)$ directly from the time-dependent reliability analysis of Section 2.3. For a maintenance action A that is a planned inspection at time t with a decision to repair if the crack depth exceeds a threshold arep, the probability of the repair outcome is $P\big(a(t) > a_{rep}\big) = \int_{a_{rep}}^{\infty} f_{a(t)}(a)\, da$, where $f_{a(t)}$ is the posterior predictive distribution of the crack depth obtain from the Bayesian updating and the crack growth model. The probability of the complementary no-repair outcome is $1 - P\big(a(t) > a_{rep}\big)$. For actions where no intervention is foreseen the probability of failure before a future time step is set to the cumulative failure probability $P_f(t + \Delta t)$ defined in Equation (8). The utility functions $U(O_i)$ are then cost values representing inspection, repair, and failure consequences as illustrated in the case study (Section 3.4).

To enact this theory in a real-time monitoring, the framework utilizes the dynamic risk thresholds of the time-dependent probability of failure ($P_f(t)$), which is calculated in Section 2.3. If the updated $P_f(t)$ stands beyond the safety limits, the system automatically announces the maintenance protocol linked. This methodology makes sure that the resources are directed on the basis of actual status of the structure which has been evolved rather than static time serving, thus minimizing unnecessary downtimes while offering safety margins throughout the wind turbine life.

3. Case study application to a floating offshore wind turbine

3.1. Reference system and structural configuration

The proposed framework is evaluated using the IEA 15 MW reference offshore wind turbine, a model developed under IEA Wind Task 37 to serve as a standard for studying the behavior of high-capacity wind energy systems [71]. With a 240-meter rotor diameter and a hub height of 150 meters, the turbine is designed to maximize energy output in deep-sea environments. It is supported by the VolturnUS-S semi-submersible floating foundation, which consists of three large outer columns arranged radially around a central column, linked by horizontal pontoons to create a robust and stable structure [72]. Stability is maintained through a catenary mooring system that combines chain and polyester rope segments. This flexible setup permits controlled movement of the platform while reducing peak loads during severe ocean conditions.

Even though the probabilistic framework is designed to be modular and can be applied to many fatigue-sensitive components (for instance, ring-flange connections and mooring lines), this analysis is focused on the tower base because it is particularly recognized as vulnerable in offshore configurations [21,73,74]. The architecture of the framework component-independent, separating the degradation physics kernel from the Bayesian updating module, allows easy adaptations to other critical subsystems. For instance, using the approach in mooring lines would require a different model; instead of the corrosion-fatigue model, it would use a chain cable degradation law while still using the same probabilistic updating and decision-making framework. Equally, scalability to larger or other turbine models is achieved by modifying environmental loading inputs and geometric parameters without affecting the core inference methodology. In Figure 2, the aerodynamic thrust, from the blades, produces bending moments that are transmitted through the tower and finally distributed at the foundation interface mentioned at the foundation interface. It has been shown that the tower base suffers from a complex combination of loads: it undergoes high amplitudes cyclic stresses due to wind turbulence and frequencies of bending moments due to hydrodynamic wave action [21,22]. On top of that, the tower base is partially submerged, which leads it into the splash zone. This environment promotes a variety of degradation mechanisms, particularly chloride-induced corrosion, which in turn initiates fatigue cracks [25]. Thus, the tower base is one of the main bottlenecks in the structure, which in turn, has an impact on the long-term performance of the floating asset.

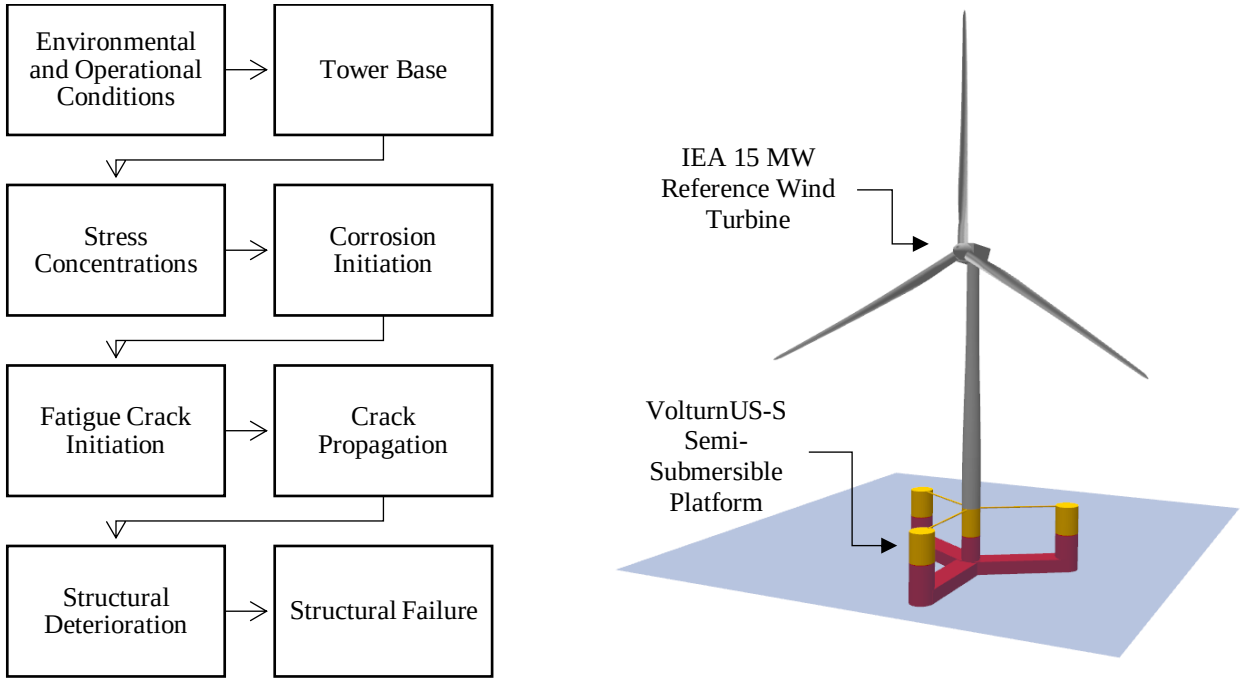

Figure 2. Visual representation of the floating offshore wind turbine system. The three-dimensional visualisation was generated by the authors using QBlade Community Edition (QBlade-CE) [76].

3.2. Operational parameters and simulation setup

The probabilistic simulation is arranged such that the tower base's operational conditions will be depicted in an exemplifying coupled load environment. The fatigue analysis adopts as an initial equivalent flaw $a_0 = 0.15$ mm, consistent with commonly reported recommendations [75]. The critical failure threshold (a_{cr}) with 82.95 mm is also set, which is the same as the thickness of the reference tower base. The environmental boundary conditions will be simulated such that it experiences a high salinity splash zone (35 PSU) with cyclic wet-dry conditions, whereas the mechanical loading will be modeled as a constant amplitude stress range of $\Delta\sigma = 50$ MPa at a frequency of 0.5 Hz, corresponding to the first fore-aft bending mode of the floating structure [72].

The Bayesian inference module is initialized by assigning prior probability distributions to the material fatigue parameters, reflecting the inherent scatter in steel crack-growth behaviour. The Paris law coefficient is represented as $C \sim \text{LogNormal}(-33.0,\ 0.4)$ (mm/cycle), and the exponent is represented as $m \sim \mathcal{N}(3.0,\ 0.15)$. To evaluate the updating capability of the framework, a sequence of synthetic crack-growth observations is used to emulate periodic inspection campaigns at 4-year intervals. Because long-term field measurements for corrosion-fatigue at floating offshore wind turbine tower bases are still scarce, synthetic observations generated from established physical crack-growth laws provide a controlled benchmark for method verification. The observations ($a_{obs} = [0.18,\ 0.38,\ 0.75,\ 1.40,\ 2.60]$ mm) are combined with measurement noise ($\sigma_{obs} = 0.5$ mm) to represent the accuracy limits of realistic non-destructive evaluation techniques. In this demonstration, the inspection method is assumed to have a high probability of detection ($PoD \approx 1.0$) for cracks larger than the initial flaw size, so that the parameter-updating mechanism can be isolated. As discussed in Section 2.3, however, the framework can incorporate technique-specific probability-of-detection curves, such as log-normal reliability functions, to represent field uncertainties including biofouling and sensor occlusion. The

probabilistic assessment is performed using 10,000 Monte Carlo simulations to propagate uncertainty through the multi-phase degradation model.

3.3. Bayesian updating and prognostic validation

The effectiveness of the probabilistic digital twin is demonstrated by the progressive refinement of the fatigue parameters m and $\ln C$ as operational observations are assimilated. As shown in Figure 3a,b, the posterior probability distributions become narrower and their central values shift as additional crack-growth data are incorporated. The change from the prior distribution to Update 1 is small, which is consistent with the early stage of crack development, where growth remains below 0.2 mm and the observations remain close to the baseline material behaviour. As damage accumulates, the Bayesian updating mechanism adjusts the parameter estimates to capture the increasingly nonlinear crack-growth response. By Update 5 (year 20), the Paris law exponent m converges around a mean value of approximately 3.15, with a more concentrated distribution than the initial prior. The logarithmic coefficient $\ln C$ also shifts from an initial mean of −33.0 to approximately −32.4, indicating a faster crack-growth rate than originally assumed. This reduction in parameter uncertainty converts broad population-level assumptions into asset-specific prognosis for the monitored tower base.

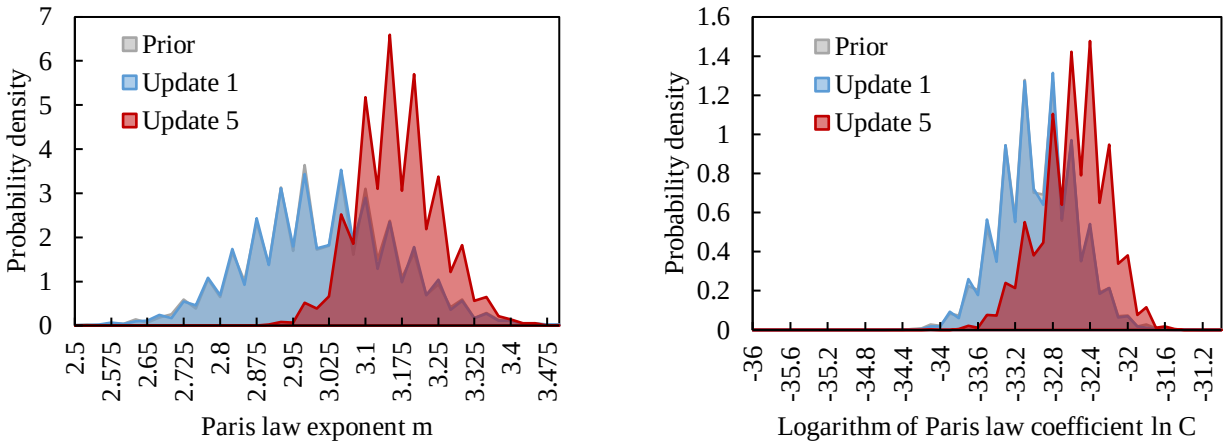

Figure 3. Evolution of posterior probability density functions for fatigue parameters: **(a)** Paris law exponent m; **(b)** Logarithm of Paris law coefficient lnC. Note: The Prior distribution is largely masked by Update 1 due to the high convergence of early-stage observations with the baseline assumptions.

The operational effect of this parameter updating is shown in Figure 4, which compares the predicted crack-growth trajectories with the inspection observations. The prior trajectory, based on generic design assumptions, predicts a crack depth of only 40.9 mm after 60 years and would therefore incorrectly suggest a large safety margin. In contrast, the Update 5 trajectory, informed by sequential observations, identifies the onset of accelerated fatigue-crack propagation. Although the observed crack depth remains approximately 3.0 mm after 20 years of operation, the updated physics-based model recognises this point as the transition into a rapidly propagating regime. The Update 5 projection therefore predicts that damage may increase from 10 mm to the critical threshold of 82.95 mm within about five years (years 20–25). This steep

increase is physically consistent with Paris law behaviour, because the stress-intensity factor range (ΔK) increases with the square root of crack depth, creating nonlinear feedback as the crack enters the macro-crack regime.

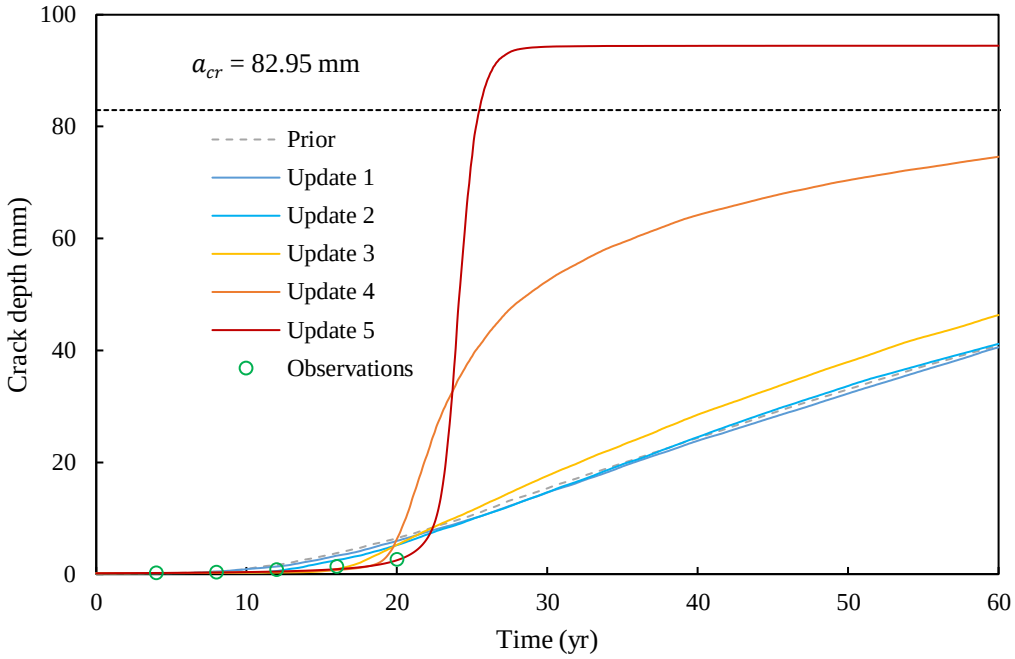

Figure 4. Comparison of crack growth trajectories between prior assumptions and Bayesian updates.

The implications of this physical degradation are further clarified through the evolution of the cumulative failure probability ($P_f(t)$), as shown in Figure 5. Over the first operational decade (Updates 1 and 2), the risk profiles do not depart substantially from the Prior baseline, yielding a flat trajectory with the forecasted failure probability at year 30 remaining below 0.15. This latency reflects the dominance of the crack initiation phase that is characterized by minimal macroscopic growth and experimental data with adequate spread to contest the design assumptions. A transition of the risk assessment is unmistakable between Update 3 and Update 4 where the probability of failure curves develop a steeper slope and shift to the left. This marks the early onset of the crack rapid propagation phase. Advancing to the final update (year 20), the model experiences its first significant update: the small source of uncertainty, and therefore, the spread of the risk profile is diminished, and the new prediction threshold exceeds the previous maximum prediction. This forecast is strongly affirmed by the performance history to date in addition to all available data supporting the crack growing at an ever-increasing rate. The probability of failure at year 25 grows from approximately 0.35 (Update 4) to nearly 1.0 (Update 5), which is broader binary evidence indicating of a high-risk plant. Inspecting the predictive inspection frequency, the fixed 4-year interval did detect this transition in risk for the current study (detection of acceleration at year 20 preceding the forecasted failure at year 24.5). However, it was noted that additional years were prematurely into the forecasted growth phase, thus other methods with an active inspection frequency such as the adaptive interval based on rise in P_f would present a more conservative but still economically viable option in plants with higher sources of uncertainty.

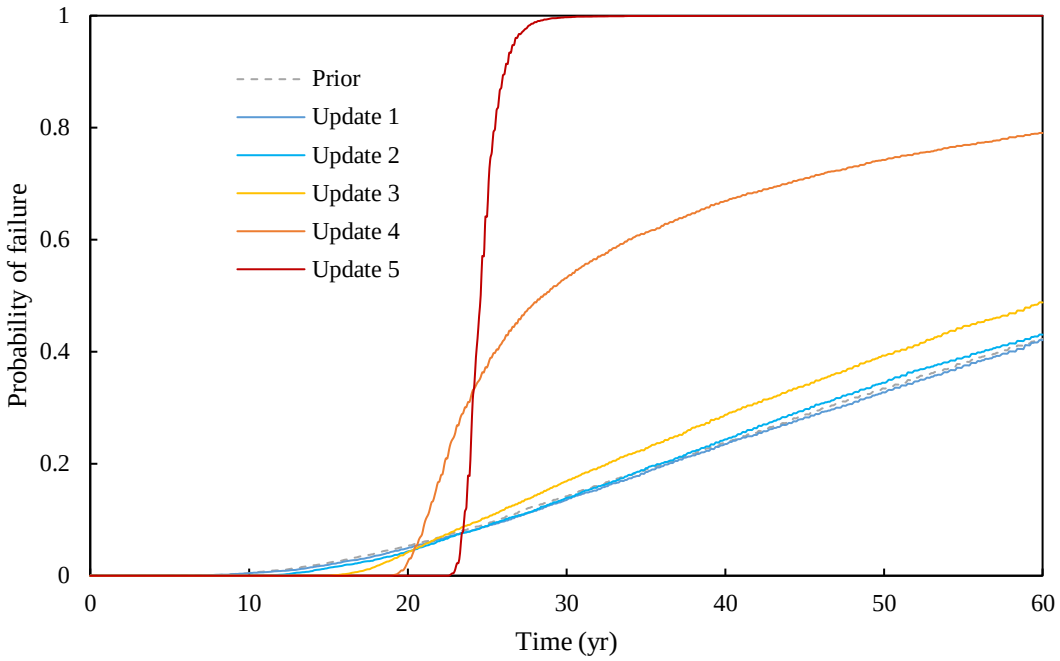

Figure 5. Temporal evolution of cumulative failure probability across Bayesian updates.

The quantification of the output from this probabilistic updating process can be found in Table 1, which illustrates the gradual enhancement of the remaining useful life estimates and their corresponding probability intervals. Crucially, the values of the remaining useful life presented reflect the projected residual service life that has been computed from the moment the update was applied (*i.e.*, the present time), and not the total accumulated life span. In the beginning, the Prior model predicts a mean of 50.3 years for the remaining useful life. On the contrary, this estimation is affected by a strong epistemic uncertainty, which is shown by a relatively wide confidence interval of 95% that covers 40 years (19.6–60 years). During the period, the digital twin receiving accelerated crack data between the updates 3 and 5, mean remaining useful life implodes, changing from 36.8 years old in 12 years to 4.8 years, which is critical, in 20 years. This alteration is trailed by a collapse of predictive variance that is noticeable; confidence interval becomes precise at last update and is stated as 3.4 years (3.4–6.8 years). The shift from a diffuse, high-uncertainty prognosis to a tightly bounded, critical alert is made possible through the relevant statistical confidence that makes justifiable the switch from passive monitoring to the active maintenance interventions which are analyzed in the next section.

Table 1. Progression of RUL estimates and 95% confidence intervals across Bayesian update stages.

Update stage	Current time (years)	Mean remaining useful life (years)	Lower CI (5%)	Upper CI (95%)
Prior	0	50.3	19.6	60
Update 1	4	46.5	16.1	56
Update 2	8	42.2	12.8	52
Update 3	12	36.8	8.7	48
Update 4	16	19.8	4.5	44
Update 5	20	4.8	3.4	6.8

3.4. Comparative analysis of maintenance strategies

To assess the economic implementation of a digital twin framework, a lifecycle analysis carried out against conventional time-based maintenance protocols was undertaken. The economic model is created with cost assumptions provided by the various industry standards for 15 MW floating assets: an inspection campaign cost (C_{insp}) is \$25,000, a minor structural repair cost (C_{rep}) is \$80,000, and a catastrophic failure consequence (C_{fail}) is \$5,000,000, which includes asset replacement as well as prolonged revenue loss. Downtime penalties were set at the level of \$750 per hour, on the basis of the lost energy share during the intervention time slots. In the simulation of the three different strategies over a 40-year span include (i) a sparse time-based strategy with a fixed 5-year inspection interval, demonstrating a minimal compliance approach; (ii) a dense time-based strategy with a two-year interval, representing a high level of conservatism by ensuring safety at all costs; and (iii) a condition-based digital twin strategy, which triggers inspections only when the probability of failure exceeds 0.1 and initiates repair when it surpasses 0.8.

The simulation's quantitative outputs, as shown in Table 2, illustrate the serious limitations of the static schedule in the regard of rising fatigue damage. The 5-year time-based sparse strategy, while enjoying a lower operational cost in the mid-term, misses the signal of the new rapidly crack propagating phase at year 22 before was a risk, at year 24.5 was shutting down (*i.e.*, a time failure to detect the defect). In total lifecycle, this approach ends over \$6.25 million due to the risk-exceedance shutdown. Meanwhile, the dense (2-year) time-based strategy achieved the goal of failing safe, catching the fault on time to repair but at a cost of efficiency; the scheme involves 13 individual inspection campaigns, which add up to a total of \$576,000 and 228 hours of operational downtime. This outcome underscores a fundamental inefficiency in conventional strategies; resources are spent inspecting intact components simply due to fixed, inflexible schedules.

Table 2. Performance of interval-based maintenance *versus* condition-based maintenance.

Strategy	Cost (\$)	Downtime (h)	Inspections	Repairs	Mandatory risk-based shutdowns
Interval-based (5 years)	6,250,000	1500	5	0	1
Interval-based (2 years)	576,000	228	13	1	0
Condition-based	202,000	96	2	1	0

In contrast, the condition-based digital twin approach achieves an effective balance between safety and cost-efficiency. By using updated risk assessments to remain inactive during crack initiation and only engaging during crack propagation, the system requires just two focused inspections and one well-timed repair. This targeted strategy lowers total lifecycle costs to \$202,000, about 64.9% less than the intensive inspection approach, while delivering identical reliability, with no failures recorded. Additionally, operational availability improves significantly, cutting downtime to only 96 hours, a 58% enhancement over the more conservative baseline. These outcomes highlight the decision module's dual role: ensuring safety while substantially improving economic performance, demonstrating that predictive risk modeling allows operators to shift from routine-based spending to proactive, risk-informed maintenance that preserves value.

4. Conclusion

This paper developed a probabilistic digital twin framework for corrosion-fatigue prognosis by integrating a multi-phase degradation model with recursive Bayesian inference to support lifecycle management of floating offshore wind turbines. The case study on the IEA 15 MW reference turbine demonstrates how the framework reduces prognostic uncertainty and informs maintenance decisions. The main findings are as follows:

(1) The Bayesian updating module corrected the overly optimistic prior projection, which estimated a benign crack depth of 40.9 mm at year 60, by identifying the onset of accelerated crack propagation at year 20 and the subsequent progression towards the critical threshold of 82.95 mm.

(2) Assimilating periodic inspection observations substantially reduced epistemic uncertainty in the remaining-useful-life estimate. The 95% confidence interval narrowed from an initial span of 40.4 years to 3.4 years after the final update.

(3) The failure-probability trajectory was sensitive to the fatigue-transition phase, increasing from 0.35 to 0.98 within one inspection interval. This behaviour indicates that the updated probability of failure can provide a clear intervention trigger under the assumed case-study conditions.

(4) Compared with a two-year fixed-interval maintenance strategy, the condition-based strategy reduced lifecycle cost by 64.9% and saved approximately USD 374,000 per turbine in the case study, while avoiding structural failures under the assumed model conditions.

(5) By avoiding redundant inspections during the crack-initiation stage, the digital-twin-guided strategy reduced operational downtime from 228 h to 96 h, equivalent to a 58% reduction. This result suggests that probabilistic monitoring can improve maintenance efficiency while maintaining risk awareness.

Several limitations remain. The current implementation uses a one-dimensional stress-intensity factor and assumes high detection reliability. Future work should incorporate mixed-mode fracture mechanics and probability-of-detection models to represent sensor limitations, as well as adaptive inspection scheduling for critical transition phases. The case study is a theoretical demonstration, so field validation with operational data is required before the predictive accuracy and transferability of the framework can be fully assessed. Although the modular structure may support application to other subsystems and turbine classes, such extension must be verified using long-term monitoring and inspection data.

Data availability statement

The data supporting the findings of this paper are available at: https://doi.org/10.5281/zenodo.20689673.

Declaration of generative AI and AI-assisted technologies

During the preparation and revision of this manuscript, the authors used DeepSeek V3 only for language polishing, grammar checking and readability improvement. The tool was not used for idea development, research design, data generation, data analysis, figure generation, interpretation of results, or the formulation of conclusions. All AI-assisted edits were reviewed and approved by the authors, who take full responsibility for the originality, accuracy and integrity of the manuscript.

Acknowledgments

The authors would like to acknowledge the financial support from National Key Research and Development Program of China (2024YFF0505400), National Natural Science Foundation of China (U24A20177), Sichuan Science and Technology Program (2025ZNSFSC1316), Qingdao Science & Technology Department Project (2511gjgg50hy), Sichuan Provincial Transportation Science and Technology Project (2024-C-18), the Fundamental Research Funds for the Central Universities (YJ202404), and China Scholarship Council (2024GSP006483 and 2024GSP006413). These supports are greatly appreciated. Any opinions, findings, and conclusions expressed in this material are those of the authors and do not necessarily reflect the views of the sponsors.

Authors' contribution

Yasmin Ali: conceptualization, data curation, formal analysis, funding acquisition, methodology, validation, writing—original draft, writing—review and editing; Ahmed Elgammal: conceptualization, funding acquisition, investigation, software, visualization, writing—original draft, writing—review and editing; Chengjun Li: funding acquisition, resources, writing—review and editing; Junlin Heng: conceptualization, funding acquisition, supervision, writing—review and editing; Kaoshan Dai: conceptualization, funding acquisition, supervision; writing—review and editing. All authors have read and agreed to the published version of the manuscript.

Conflicts of interest

The authors declare that they have no known competing financial interests or personal relationships that could have appeared to influence the work reported in this paper.

References

[1] Long Y, Chen Y, Xu C, Li Z, Liu Y, *et al.* The role of global installed wind energy in mitigating CO_2 emission and temperature rising. *J. Cleaner Prod.* 2023, 423:138778.

[2] Zhang Z, Jiao B, Sun H, Lin H, Shi J. Collective and individual blade pitch control strategy for floating wind turbines based on improved ALO and fractional order PIDD2. *Ocean Eng.* 2025, 341:122851.

[3] Ribeiro JA, Ribeiro BA, Pimenta F, Tavares SMO, Zhang J, *et al.* Offshore wind turbine tower design and optimization: A review and AI-driven future directions. *Appl. Energy* 2025, 397:126294.

[4] Li H, D áz H, Soares CG. A failure analysis of floating offshore wind turbines using AHP-FMEA methodology. *Ocean Eng.* 2021, 234:109261.

[5] Hu Y, Wang J, Chen M, Li Z, Sun Y. Load mitigation for a barge-type floating offshore wind turbine via inerter-based passive structural control. *Eng. Struct.* 2018, 177:198–209.

[6] Nie D, Yang Y, Li S, Yu J, Bashir M, *et al.* Investigation of mooring breakage impact on dynamic responses of a 15 MW floating offshore wind turbine. *Ocean Eng.* 2024, 311:118996.

[7] Hu D, Zheng Z, Xia F, Lai W, Chen N. Impacts and mechanisms of wave motion on aerodynamic characteristics of FOWTs via overlapping grid CFD. *Ocean Eng.* 2026, 346:123847.

[8] Wei B, Zhang Z, Xiao F, Fang F, Qin S. Adaptive backstepping-sliding mode control strategy for robust MPPT of floating offshore wind turbines. *Ocean Eng.* 2025, 342:122735.
[9] Bi C, Zhang Y, Ma C, Cui S. Experimental study on the hydrodynamic responses of a novel platform integrating vertical-axis wind turbine with a fish cage in regular waves. *Aquacult. Eng.* 2025, 111:102585.
[10] Angliviel De La Beaumelle N, Azevedo IML. Techno-economic assessment of floating offshore wind in California. *Environ. Res. Lett.* 2025, 20:114066.
[11] Poulsen T, Hasager C, Jensen C. The role of logistics in practical levelized cost of energy reduction implementation and government sponsored cost reduction studies: day and night in offshore wind operations and maintenance logistics. *Energies* 2017, 10:464.
[12] Costa ÁM, Orosa JA, Vergara D, Fernández-Arias P. New tendencies in wind energy operation and maintenance. *Appl. Sci.* 2021, 11:1386.
[13] Taylor JW, Jeon J. Probabilistic forecasting of wave height for offshore wind turbine maintenance. *Eur. J. Oper Res.* 2018, 267:877–890.
[14] Scheu M, Matha D, Schwarzkopf MA, Kolios A. Human exposure to motion during maintenance on floating offshore wind turbines. *Ocean Eng.* 2018, 165:293–306.
[15] Peng Z, Sun S, Tong L, Fan Q, Wang L, *et al.* Optimization of offshore wind farm inspection paths based on K-means-GA. *PLoS One* 2024, 19:e0303533.
[16] Dalgic Y, Lazakis I, Dinwoodie I, McMillan D, Revie M. Advanced logistics planning for offshore wind farm operation and maintenance activities. *Ocean Eng.* 2015, 101:211–26.
[17] Dao CD, Kazemtabrizi B, Crabtree CJ, Tavner PJ. Integrated condition-based maintenance modelling and optimisation for offshore wind turbines. *Wind Energy* 2021, 24:1180–1198.
[18] Turnbull A, Carroll J. Cost benefit of implementing advanced monitoring and predictive maintenance strategies for offshore wind farms. *Energies* 2021, 14:4922.
[19] Zhou P, Yin P. An opportunistic condition-based maintenance strategy for offshore wind farm based on predictive analytics. *Renewable Sustainable Energy Rev.* 2019, 109:1–9.
[20] Luo J, Luo X, Ma X, Zan Y, Bai X. An integrated condition-based opportunistic maintenance framework for offshore wind farms. *Reliab. Eng. Syst. Saf.* 2025, 256:110701.
[21] Li H, Hu Z, Wang J, Meng X. Short-term fatigue analysis for tower base of a spar-type wind turbine under stochastic wind-wave loads. *Int. J. Nav. Archit. Ocean Eng.* 2018, 10:9–20.
[22] Jiang Y, Chen P, Wang S, Cheng Z, Xiao L. Dynamic responses of a 5 MW semi-submersible floating vertical-axis wind turbine: A model test study in the wave basin. *Ocean Eng.* 2024, 296:117000.
[23] Yan X, Yan L, Kang S, Qi X, Xu M, *et al.* Corrosion behavior and electrochemical corrosion of a high manganese steel in simulated marine splash zone. *Mater. Res. Express* 2021, 8:126507.
[24] Yan X, Kang S, Xu M, Li P. Corrosion product film of a medium-mn steel exposed to simulated marine splash zone environment. *Materials* 2021, 14:5652.
[25] Xu K, Zhang M, Shao Y, Gao Z, Moan T. Effect of wave nonlinearity on fatigue damage and extreme responses of a semi-submersible floating wind turbine. *Appl. Ocean Res.* 2019, 91:101879.
[26] Zhu F, Yeter B, Brennan F, Collu M. Time-domain fatigue reliability analysis for floating offshore wind turbine substructures using coupled nonlinear aero-hydro-servo-elastic simulations. *Eng. Struct.* 2024, 318:118759.

[27] Chen Z, Jafarzadeh S, Zhao J, Bobaru F. A coupled mechano-chemical peridynamic model for pit-to-crack transition in stress-corrosion cracking. *J. Mech. Phys. Solids* 2021, 146:104203.
[28] Wei Y, Li Y, Lai J, Zhao Q, Yang L, *et al.* Analysis on corrosion fatigue cracking mechanism of 17-4PH blade of low pressure rotor of steam turbine. *Eng. Fail. Anal.* 2020, 118:104925.
[29] Igwemezie V, Mehmanparast A. Waveform and frequency effects on corrosion-fatigue crack growth behaviour in modern marine steels. *Int. J. Fatigue* 2020, 134:105484.
[30] Tu W, Yue J, Xie H, Tang W. Fatigue crack propagation behavior of high-strength steel under variable amplitude loading. *Eng Fract. Mech* 2021, 247:107642.
[31] Zhang J, Muys L, De Tender S, Micone N, Hertelé S, *et al.* Constraint corrected cycle-by-cycle analysis of crack growth retardation under variable amplitude fatigue loading. *Int. J. Fatigue* 2019, 125:199–209.
[32] Calderon-Uriszar-Aldaca I, Briz E, Biezma MV, Puente I. A plain linear rule for fatigue analysis under natural loading considering the coupled fatigue and corrosion effect. *Int. J. Fatigue* 2019, 122:141–151.
[33] Bolton JD, Redington ML. The effects of saline aqueous corrosion on fatigue crack growth rates in 316 grade stainless steels. *Int. J. Fatigue* 1983, 5:155–63.
[34] Dong Y, Garbatov Y, Guedes Soares C. Review on uncertainties in fatigue loads and fatigue life of ships and offshore structures. *Ocean Eng.* 2022, 264:112514.
[35] Liu X, Lu D. Uncertainties quantification of fatigue load mixture model using hierarchical Bayesian models. *Int. J. Fatigue* 2023, 174:107734.
[36] Cui S, Li J, Chen S, Wang C, Cheng L, *et al.* An approach for fatigue damage estimation under broadband non-Gaussian random loadings based on the Johnson transformation model. *Appl. Ocean Res.* 2024, 148:104039.
[37] Ćorak M, Mikulić A, Katalinić M, Parunov J. Uncertainties of wave data collected from different sources in the Adriatic Sea and consequences on the design of marine structures. *Ocean Eng.* 2022, 266:112738.
[38] Khanna A, Kotousov A. The potential for structural simulation to augment full scale fatigue testing: a review. *Prog. Aerosp. Sci.* 2020, 121:100641.
[39] Moradi M, Broer A, Chiachío J, Benedictus R, Loutas TH, *et al.* Intelligent health indicator construction for prognostics of composite structures utilizing a semi-supervised deep neural network and SHM data. *Eng. Appl. Artif. Intell.* 2023, 117:105502.
[40] Papadopoulos DI, Giannakopoulos G, Karkaletsis V, Rekatsinas C. A data-lean machine learning approach for damage extent estimation and classification in composite structures under multiple failure modes. *Mach. Learn.: Sci. Technol.* 2025, 6:035042.
[41] Bao Y, Li H. Machine learning paradigm for structural health monitoring. *Struct. Health Monit.* 2021, 20:1353–1372.
[42] Sun C, Chen Y, Cheng C. Imputation of missing data from offshore wind farms using spatio-temporal correlation and feature correlation. *Energy* 2021, 229:120777.
[43] Han T, Xie W, Pei Z. Semi-supervised adversarial discriminative learning approach for intelligent fault diagnosis of wind turbine. *Inf. Sci.* 2023, 648:119496.

[44] Cevasco D, Koukoura S, Kolios AJ. Reliability, availability, maintainability data review for the identification of trends in offshore wind energy applications. *Renewable Sustainable Energy Rev.* 2021, 136:110414.
[45] Moghadam FK, Nejad AR. Online condition monitoring of floating wind turbines drivetrain by means of digital twin. *Mech. Syst. Signal Process.* 2022, 162:108087.
[46] Stadtmann F, Rasheed A, Kvamsdal T, Johannessen KA, San O, *et al.* Digital twins in wind energy: emerging technologies and industry-informed future directions. *IEEE Access* 2023, 11:110762–110795.
[47] Ali Y, Elgammal A, Heng J, Dai K, Saudi GN, *et al.* Insights into corrosion-fatigue deterioration in offshore wind turbine structures through digital twin applications. *Ocean Eng.* 2026, 343:123514.
[48] Yucesan YA, Viana FAC. Physics-informed digital twin for wind turbine main bearing fatigue: quantifying uncertainty in grease degradation. *Appl. Soft Comput.* 2023, 149:110921.
[49] VanDerHorn E, Wang Z, Mahadevan S. Towards a digital twin approach for vessel-specific fatigue damage monitoring and prognosis. *Reliab. Eng. Syst. Saf.* 2022, 219:108222.
[50] Ritto TG, Rochinha FA. Digital twin, physics-based model, and machine learning applied to damage detection in structures. *Mech. Syst. Signal Process.* 2021, 155:107614.
[51] Ali Y, Dai K, Elgammal A, Luo Y, Heng J, *et al.* AI-driven digital twin for corrosion-fatigue management and opportunistic maintenance in offshore wind turbines. *Wind Struct.* 2025, 41:393–411.
[52] Ma J, Bai N, Zhou Y, Lan C, Li H, *et al.* Generalized hierarchical Bayesian inference for fatigue life prediction based on multi-parameter Weibull models. *Int. J. Fatigue* 2022, 162:106948.
[53] Rabiei M, Modarres M. Quantitative methods for structural health management using *in situ* acoustic emission monitoring. *Int. J. Fatigue* 2013, 49:81–89.
[54] Simpson HA, Chatzi EN, Chatzis MN. A comparison of deterministic and Bayesian model updating frameworks for identifying offshore wind turbine foundation parameters. *J. Sound Vib.* 2026, 625:119575.
[55] Adedipe T, Shafiee M, Zio E. Bayesian network modelling for the wind energy industry: an overview. *Reliab. Eng. Syst. Saf.* 2020, 202:107053.
[56] Xu T, Zhang X, Sun W, Wang B. Intelligent operation and maintenance of wind turbines gearboxes via digital twin and multi-source data fusion. *Sensors* 2025, 25:1972.
[57] Zhang J, Heng J, Dong Y, Baniotopoulos C, Ali Y. A digital twinning framework for intelligent operation and maintenance of floating offshore wind turbines under corrosion-fatigue. *IOP Conf. Ser.: Earth Environ. Sci.* 2025, 1552:012023.
[58] Zheng T, Heng J, Song J, Zhou D, Luo Y, *et al.* Prognostic digital twinning of lattice-tubular hybrid wind turbine towers exposed to deterioration. *Structures* 2025, 79:109461.
[59] Jyeniskhan N, Shomenov K, Ali MH, Shehab E. Exploring the integration of digital twin and additive manufacturing technologies. *Int. J. Lightweight Mater. Manuf.* 2024, 7:860–881.
[60] VanDerHorn E, Mahadevan S. Digital Twin: generalization, characterization and implementation. *Decis. Support Syst.* 2021, 145:113524.
[61] Liao X, Li Y, Qiang B, Wu J, Yao C, *et al.* An improved crack growth model of corrosion fatigue for steel in artificial seawater. *Int. J. Fatigue* 2022, 160:106882.
[62] Syrotyuk AM, Babii AV, Barna RA, Leshchak RL, Marushchak PO. Corrosion-fatigue crack-growth resistance of steel of the frame of a sprayer boom. *Mater. Sci.* 2021, 56:466–471.

[63] Liu Y, Mahadevan S. Probabilistic fatigue life prediction using an equivalent initial flaw size distribution. *Int. J. Fatigue* 2009, 31:476–487.

[64] Anderson TL. *Fracture Mechanics: Fundamentals and Applications*, 4th ed. Boca Raton: CRC Press, 2017.

[65] Zhang J, Heng J, Dong Y, Baniotopoulos C, Yang Q. Coupling multi-physics models to corrosion fatigue prognosis of high-strength bolts in floating offshore wind turbine towers. *Eng. Struct.* 2024, 301:117309.

[66] Myshkov P, Julier S. Posterior distribution analysis for bayesian inference in neural networks. In *Proceedings of the Workshop Bayesian Deep Learn*ing *(NIPS) 2016*, Barcelona, Spain, December 5–10, 2016.

[67] Kim H, Lee D. Bayesian decision analysis of nondestructive inspection threshold for structural reliability analysis. *NDT & E Int.*2026, 160:103674.

[68] Amirafshari P, Kolios A. Estimation of weld defects size distributions, rates and probability of detections in fabrication yards using a Bayesian theorem approach. *Int. J. Fatigue* 2022, 159:106763.

[69] Mazzatura I, Casas JR, Salvatore W, Caprili S. Reliability of ultrasonic tomography in detecting grouting defects in post-tensioned structures by PoD curves. *Eng. Struct.* 2024, 302:117352.

[70] Pedersen TI, Vatn J. Optimizing a condition-based maintenance policy by taking the preferences of a risk-averse decision maker into account. *Reliab. Eng. Syst. Saf.* 2022, 228:108775.

[71] Gaertner E, Rinker J, Sethuraman L, Zahle F, Anderson B, *et al*. Definition of the IEA Wind 15-Megawatt Offshore Reference Wind Turbine. 2020. Available: https://doi.org/10.2172/1603478 (accessed on 4 April 2025).

[72] Allen C, Viscelli A, Dagher H, Goupee A, Gaertner E, *et al.* Definition of the UMaine volturnUS-S reference platform developed for the IEA wind 15-megawatt offshore reference wind turbine. 2020. Available: https://doi.org/10.2172/1660012 (accessed on 4 April 2025).

[73] Liu DP, Ferri G, Heo T, Marino E, Manuel L. On long-term fatigue damage estimation for a floating offshore wind turbine using a surrogate model. *Renew Energy* 2024, 225:120238.

[74] Li X, Zhang W. Long-term fatigue damage assessment for a floating offshore wind turbine under realistic environmental conditions. *Renew Energy* 2020, 159:570–584.

[75] Zhou H, Shi G, Wang Y, Chen H, De Roeck G. Fatigue evaluation of a composite railway bridge based on fracture mechanics through global–local dynamic analysis. *J. Constr. Steel Res.* 2016, 122:1–13.

[76] Marten D. QBlade: a modern tool for the aeroelastic simulation of wind turbines. Doctoral Thesis, Berlin Institute of Technology, 2020.